Interactions of *β*-Helical Antifreeze Protein Mutants with Ice

Maya Bar,*,[†] Yeliz Celik,[‡] Deborah Fass,[†] and Ido Braslavsky[‡]

*Department of Structural Biology, Weizmann Institute of Science, Rehovot 76100, Israel, and
Department of Physics and Astronomy, Ohio University, Athens, Ohio 45701*

Received January 17, 2008; Revised Manuscript Received April 3, 2008

ABSTRACT: The fold of the *β*-helical antifreeze protein from *Tenebrio molitor* (TmAFP) proved to be surprisingly tolerant of multiple amino acid substitutions, enabling the construction of a panel of mutants displaying grids of single amino acid types in place of the threonines on the ice-binding face. These mutants, maintaining the regularity of amino acid spacing found in the wild-type protein but with different functional groups on the surface, were tested for antifreeze activity by measuring thermal hysteresis and observing ice grown in their presence. We found that no mutant exhibited the dramatic activity of the wild-type version of this hyperactive antifreeze protein. However, mutants containing four valines or tyrosines in place of the threonines in the center of the TmAFP ice-binding face showed residual thermal hysteresis activity and had marked effects on ice crystal morphology. The results are discussed in the context of a two-stage model for the absorption−inhibition mechanism of antifreeze protein binding to ice surfaces.

Introduction

Antifreeze proteins (AFPs), also known as thermal hysteresis proteins, ice-structuring proteins, and ice-binding proteins, have evolved in a variety of cold-adapted organisms to prevent ice injuries at subzero temperatures. These proteins maintain the body fluid of the organism in a liquid state by noncolligative depression of the freezing temperature, resulting in a separation between the melting and the freezing points, termed thermal hysteresis (TH). In addition to depressing the freezing point, AFPs reshape ice crystals when seed crystals are supercooled in their presence. This effect on ice crystal morphology is used to study interactions of AFPs with ice surfaces.

AFPs from various organisms have been identified and classified by molar TH activity. According to this classification, AFPs can be divided into two groups, the moderately active and the hyperactive. The first group is characterized by TH of 0.5 to 1.0 °C at millimolar protein concentrations.[1] The hyperactive AFPs have TH activity 2 orders of magnitudes higher, reaching similar TH values at tens of micromolar concentrations and up to 6 °C at millimolar concentrations.[2–4] AFPs are markedly different in sequence and structure, even within each TH activity group. For example, type I AFP is a repetitive, small, alanine-rich, amphipathic α-helix containing four regularly spaced threonine residues; the lectin-like type II AFP and the type III AFPs are nonrepetitive globular proteins; the antifreeze glycoproteins are composed of repeats of Ala-Ala-Thr, with disaccharide moieties decorating the Thr side chains.[5] All these proteins belong to the moderately active AFPs and have similar specific and maximal TH activities.[1] Only a few hyperactive antifreeze proteins are known, including two nonhomologous *β*-helical proteins from insects,[2,4,6] an elongated, Ala-rich, α-helical fish AFP,[3,7] a Gly-rich AFP from snow flea,[8] and a calcium-dependent bacterial AFP predicted to have a third class of *β*-helical structure.[9]

The commonly held theory for how AFPs depress freezing is the adsorption−inhibition mechanism.[10–13] According to this mechanism, AFPs adsorb to the surface of a growing ice crystal and poison the continuity of the ice lattice such that additional water molecules are incorporated only between the adsorbed protein molecules. Thus, the curvature of the ice crystal surface increases, and further growth is prevented in a certain temperature range below the bulk equilibrium melting point (the "hysteresis gap") by the Gibbs−Thomson effect. When the nonequilibrium freezing temperature is reached, the crystal grows rapidly in an explosive manner.[1] However, this theory, in its original manifestation, does not account for several experimental observations. For example, the observed protein concentration dependence of TH activity remains to be reconciled with a model that appears to involve irreversible binding. In addition, this theory does not address the enormous discrepancies between different AFPs in activity, protein architecture, and moieties involved in ice recognition. Furthermore, a transition layer about a nanometer thick[14] in which the molecular order gradually increases between bulk liquid water and ice precludes, according to some researchers, the possibility for a simple, direct attachment of protein to ice.[15] Some of these issues have been attended to in kinetic models based either on reversible[16] or irreversible[12] adsorption of AFP molecules to ice, or even a combination of the two.[17]

A large number of biochemical, biophysical, and structural studies have been conducted to elucidate the mechanism by which AFPs bind to specific planes of ice. It is established that shape complementarity between AFPs and the ice lattice is crucial for ice binding by both moderately active and hyperactive AFPs.[18–22] However, the underlying forces that promote binding are not completely understood. Early studies focusing on the α-helical winter flounder type I AFP suggested that hydrogen bonds between Asp, Asn, and Thr side chains projecting from a hydrophilic side of the helix and oxygen atoms on specific ice planes provide the driving force for binding.[23–25] Knight et al. proposed that the Thr side chain hydroxyl groups occupy oxygen-atom sites in the top layer of the ice lattice, maximizing the number and strength of hydrogen bond interactions between the AFP polar residues and the ice crystal.[20] However, amino acid substitutions of the four Thr residues located at the edge of the hydrophilic face, adjacent to a rank of conserved Ala residues, raised doubts about the centrality of hydrogen bonding in the AFP ice-binding mechanism.[26–28] When Thr residues were replaced with Val, which is sterically equivalent to Thr but lacks

* Corresponding author. Tel: +972-8-934-3745; fax: +972-8-934-4136; e-mail: maya.bar@weizmann.ac.il.
† Weizmann Institute of Science.
‡ Ohio University.

the side chain hydroxyl and instead has another methyl group, only a minor loss of activity was observed. In contrast, substitution to Ser, which preserves the side chain hydroxyl, had a more detrimental effect on TH activity,[26–28] suggesting that hydrophobic interactions and van der Waals forces contribute significantly to ice recognition by AFPs. Further mutagenesis studies showed that the Ala residues adjacent to the four Thr residues are crucial for TH activity, leading to the conception that protein–ice interactions occur through this Ala-rich face and neighboring Thr residues.[29] Similar results were obtained for a different type I AFP from shorthorn sculpin.[30] Furthermore, a solution structure of type III AFP from eel pout suggested that nonpolar residues contribute significantly to the good steric match between the ice-binding face of the protein and the ice lattice.[31]

The hyperactive AFPs, being considerably more active than the fish AFPs mentioned above, might bind to ice by a different mechanism. Two experimentally determined structures of hyperactive AFPs are available to date, the spruce budworm AFP (sbwAFP)[22] and TmAFP.[21] Both sbwAFP and TmAFP are β-helices, providing a model for studying ice recognition properties of AFPs that is structurally and functionally distinct from type I. TmAFP is a parallel β-helix composed of 7 repeats of 12 amino acids. The motif Thr-Cys-Thr (TCT) from each repeat makes a flat β-sheet on one side of the β-helix. The side chains of the Thr residues from this motif are regularly spaced, forming a two-dimensional array of hydroxyl and methyl groups (Figure 1A,B).[21] The spatial arrangement of these functional groups, together with a file of bound water molecules, matches almost perfectly the atomic organization on the primary prism plane (perpendicular to the *a*-axis) and, though to a lesser extent, the basal plane of ice.[21]

The excellent geometrical fit between TmAFP and the ice lattice implies that TmAFP binds to ice through the array of threonines, and single site-directed mutagenesis studies confirmed this hypothesis.[32] Accordingly, the TCT repeats of sbwAFP were also proposed to be responsible for ice recognition.[22] However, it remains to be determined whether hydrophobic interactions promote ice recognition by these insect AFPs, as observed in the fish counterparts, or whether hydrogen bonds between Thr hydroxyls and the top ice layer are dominant. To compare the importance of hydrogen bonds and hydrophobic effects for ice recognition by TmAFP, and to assess the importance of the wild-type threonines in binding, we tested a series of TmAFP multisite mutants in which blocks of the Thr residues forming the ice-binding grid were replaced by other amino acid types. In each mutant, either 8 or the central 4 of the 11 Thr residues from the TmAFP ice recognition face were substituted simultaneously with one of the amino acids asparagine (N), histidine (H), tyrosine (Y), or valine (V) (Figure 1). This approach maintains, at least in part, the uniform and repetitive arrangement of a specific functional group projecting from the β-helix that is hypothesized to be important in the activity of the native protein. These mutants were first synthesized to probe the tolerance of the TmAFP fold, rather than function, to mutation;[33] substitutions for the native threonines were chosen for their varied β-sheet propensities, sizes, and chemical properties. With respect to function, the Asn and His mutants provide groups potentially available for hydrogen bonding with the ice surface. The Tyr mutants retain the hydroxyl group, and the Val mutants retain the size, shape, and γ-methyl group of Thr. We show that, while the contribution of the native Thr residues to TH activity is much more pronounced for TmAFP than previously observed for type I
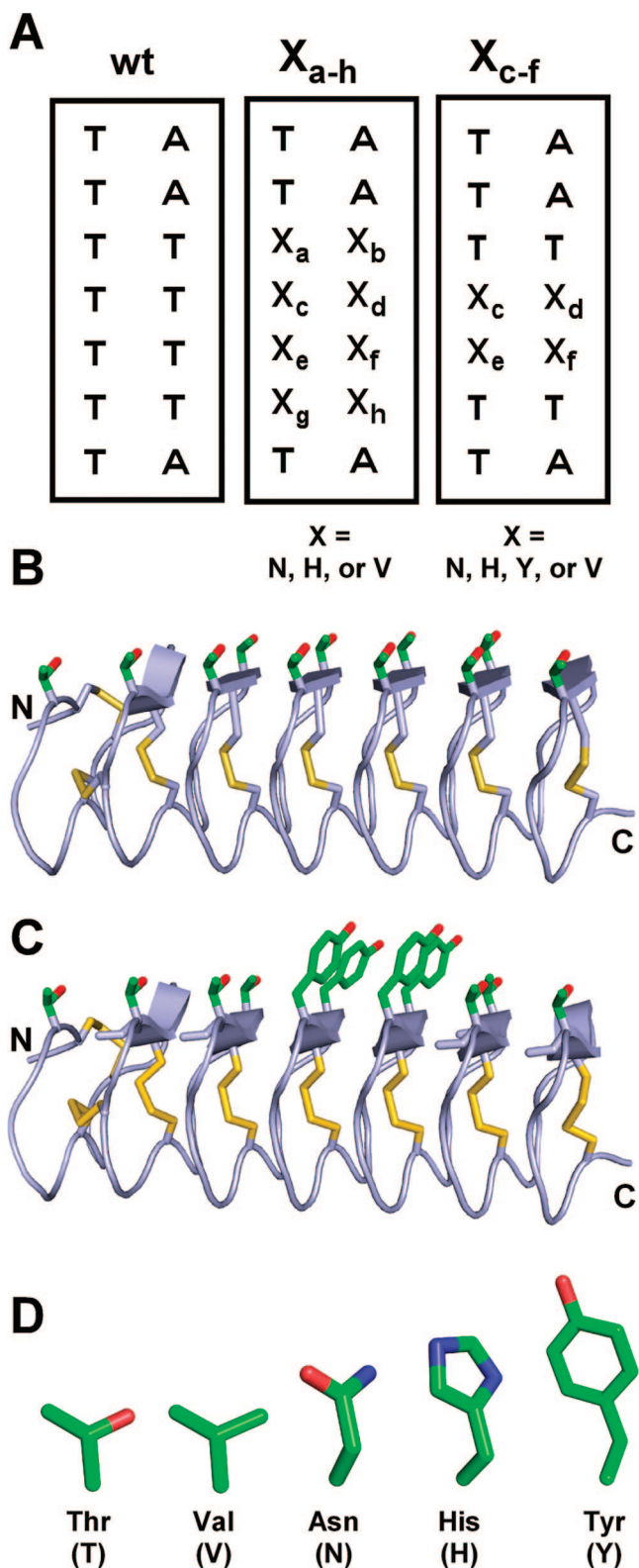

Figure 1. TmAFP structure and mutation design. (A) TmAFP ice-binding face mutations. Left, the 2 × 7 grid of the wild-type TmAFP ice-binding face with files of 7 and 4 threonine residues. Middle and right, mutation positions in the $X_{a–h}$ and $X_{c–f}$ TmAFP variants. (B) Ribbon diagram of the TmAFP structure[21] with cysteine and ice-binding threonine side chains shown as sticks. (C) A ribbon model of $Y_{c–f}$ showing the mutated ice-binding face (obtained using the SWISS_MODEL server[34]). (D) Representation of the side chains of amino acids used for mutagenesis. Atoms are colored by type (carbon, green; nitrogen, blue; oxygen, red; sulfur, yellow). Panels B–D were prepared using Pymol (DeLano Scientific LCC, San Francisco, CA).

AFPs from fish, some activity is retained when blocks of Thr are mutated to Val or Tyr. This residual activity gives insight into the interactions involved in ice recognition by hyperactive insect AFPs.

Experimental Details

Expression and Purification of TmAFP and Mutants. Wild-type TmAFP and all mutants were expressed and purified according to published protocol.[35] Briefly, proteins were expressed in the Origami B (DE3) plysS *Escherichia coli* strain (Merck KGaA, Darmstadt, Germany), purified on Ni-NTA agarose beads (Qiagen, N.V., Venlo, Netherlands), and digested with TEV protease.[36] Digested protein was reapplied on Ni-NTA, and unbound fractions were purified by reversed phase high performance liquid chromatography (HPLC). Protein concentrations were determined by amino acid analysis or using the BCA kit (Pierce, Rockford, IL). The oxidation state of each protein was verified by electrospray mass spectrometry and Ellman's assay. Folding of mutants was analyzed by circular dichroism (CD), 1D and 2D NMR spectroscopies.[33]

Reference Proteins. Bovine serum albumin (BSA) was purchased from Sigma-Aldrich (St. Louis, MO). Thioredoxin (Trx) was prepared as described.[37] Maltose binding protein (MBP) was obtained from TEV cleavage of MBP-His$_6$-TEV-TmTHP constructs[33] and purified as follows. After the second step of Ni-NTA purification of TmAFP or mutants, beads were washed thoroughly, and bound MBP was eluted. Protein purity was verified by SDS polyacrylamide gel electrophoresis. If residual uncleaved construct was detected by gel, TEV proteolysis was repeated until complete digestion was obtained. The MBP in our assays contains a carboxy-terminal His$_6$ tag. All stock solutions were dialyzed against 20 mM ammonium carbonate buffer (pH 8) and frozen at −20 °C until needed.

Experimental Equipment. Thermal hysteresis, ice crystal morphology, and ice growth rates were determined using a homemade nanoliter osmometer designed according to Chakrabartty et al.[38] Briefly, a gold-coated brass sample holder (0.8 cm diameter) containing six sample wells (0.5 mm diameter) was placed in thermal contact with a custom-built temperature-controlled stage. The thermoelectric units of the stage and a thermistor that measures the temperature in the vicinity of the sample holder were connected to a temperature controller (Newport model 3040, Irvine, CA) to allow delicate control of the temperature around the sample holder in the range of room temperature to −40 °C, with 0.01 °C precision. An external water circuit was connected to the stage to remove heat from the cooling units, and dry air flow was applied to avoid humidity around the sample holder. The stage was placed under an Olympus BH2 microscope, and samples were observed through a 50× Nikon objective lens and recorded using a Sony CCD-IRIS video camera directly into a PC harddrive via a video frame grabber device (IMAQ-PCI-1407, National Instruments). The system was controlled by an interface developed mainly by I.B. in a LabVIEW environment.[39] Before each experiment, sample wells were filled with immersion oil, and a sample droplet of typically 0.5 nL (100 μm diameter) was placed in the center of the oil to allow uniform heat dispersion around the sample.

Thermal Hysteresis Assays. To measure the equilibrium melting temperature (T_m) and the hysteresis freezing point accurately, it is necessary to obtain a small single ice crystal, such that changes in the salinity of the droplet are minimized. The samples were flash-frozen (typically between −27 and −35 °C) and heated until one ice crystal was left. The single crystal was melted to the smallest size practically possible (typically 10 μm along the *a*-axis for wild-type TmAFP and V$_{c-f}$, and 15–20 μm along the *a*-axis for all other mutants), and the melting temperature was determined as the lowest temperature at which this crystal melted. At the final size, the solution was supercooled to ∼0.02 °C below T_m, and the crystal was left for a time period of 10 min. Afterward, the temperature was lowered by 0.01 °C in constant time lapse with equilibration period at every temperature. Short equilibration times of 4 s were used in experiments with V$_{c-f}$ to avoid overgrowth of the crystals, which continued to grow during measurements. The same short equilibration times were used with wild-type TmAFP to shorten the experimental times at the high range of TH activity. For all other proteins, equilibration times of 30 s were used to allow more accurate determination of the temperatures, as required to measure TH values close to zero. The TH activity of wild-type TmAFP

was comparable for both high (−0.01 °C per 4 s) and low (−0.01 °C per 15 s) cooling rates. The hysteresis freezing point was determined as the temperature of "burst," when a sudden rapid growth of the crystal was observed. All experiments were performed in 20 mM ammonium carbonate buffer (pH 8) and repeated at least four times. Thermal hysteresis was determined as the average difference between the melting and freezing points of each ice crystal.

Growth Rate Assays. Growth rates were measured by monitoring single ice crystals at a constant supercooling temperature. For V$_{c-f}$, growth was measured along the *a*- and *c*-axes. For all other mutants growth was measured in the direction of the *a*-axis, assuming that this axis is parallel to the face of the disk-shaped ice crystals. The time scale of each experiment varied according to the crystal growth rate in the presence of each TmAFP variant. For V$_{c-f}$ measurements at temperatures close to T_m, crystals were monitored for minutes to allow sufficient growth for detection. In all other cases, growth was measured on the time scale of seconds. The size of the ice crystal at each time point was determined by direct measurement on the screen. The magnification factor was determined by measuring the size of the screen image of a 10 μm ladder positioned at the sample plane. Attempts were made to measure growth rates from crystal axes lying nearly parallel to the screen; if crystals appeared to rotate during measurement, these data were discarded. All experiments contained 1 mg/mL protein (∼0.11 mM) in 20 mM ammonium carbonate buffer (pH 8).

Results

Design and Preparation of TmAFP Mutants. The ice-binding face of TmAFP consists of 11 Thr residues arranged in an array of two parallel files of seven and four residues (Figure 1A,B). To investigate the importance of the hydrophobic and hydrophilic aspects of the Thr grid for ice binding, and to determine the extent to which grids of non-Thr residues could substitute for the wild-type Thr array, we used two series of TmAFP mutants. In the X$_{c-f}$ series, four residues were substituted in the center of the Thr array, forming a two-by-two grid of Asn, His, Val, or Tyr (mutants N$_{c-f}$, H$_{c-f}$, V$_{c-f}$, and Y$_{c-f}$, respectively) with four remaining native Thr residues upstream and three downstream. In the X$_{a-h}$ mutant series, eight Thr residues from the array were replaced, forming the mutants N$_{a-h}$, H$_{a-h}$, and V$_{a-h}$ (Figure 1). These mutants were designed to replace a significant portion of the TmAFP ice-binding face, and only a single native Thr remains downstream and two upstream of the novel two-by-eight grid. We note that a Y$_{a-h}$ mutant was also prepared but was not analyzed in detail due to poor solubility.

All TmAFP mutants were expressed and purified following the protocol used for the wild-type preparation[35] with minor modifications made as necessary for the H$_{c-f}$ and H$_{a-h}$ mutants.[33] After reversed-phase HPLC purification, protein identity was confirmed by electrospray mass spectrometry, and SDS−PAGE analysis was used to verify purity. The proteins were shown to be oxidized using Ellman's assay, and CD, 1D ^{1}H NMR, and 2D HOHAHA spectroscopies were performed to assess their folding. A detailed structural analysis of the TmAFP mutants is reported elsewhere.[33] In essence, all mutants tested in this study were shown to be monomers in solution and to maintain the overall fold of wild-type TmAFP. The 2D HOHAHA spectra of the X$_{a-h}$ mutants showed some line broadening and some areas of high background level, indicative of the presence of some unfolded or misfolded material. The improperly folded fraction may be either a part of each molecule or a part of the population of molecules. The 2D HOHAHA spectra of all mutants of the X$_{c-f}$ series indicated that these proteins are folded. Specifically, the chemical shifts of the backbone amides of the mutated positions were similar to those of the corresponding Thr residues in the wild-type protein. CD spectra of V$_{a-h}$, V$_{c-f}$, and Y$_{c-f}$ were almost
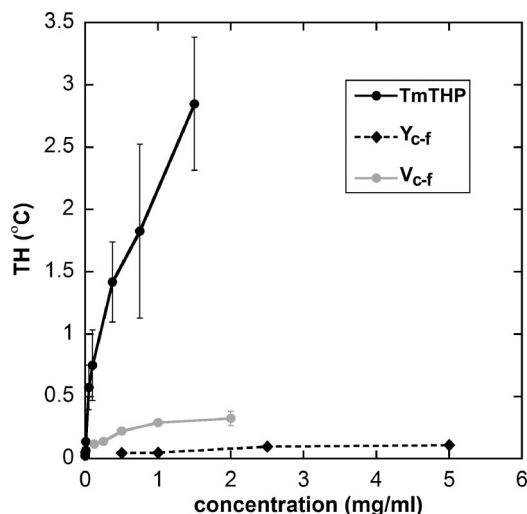
Figure 2. Concentration dependence of the thermal hysteresis activity of TmAFP and mutants. V_{c-f} and Y_{c-f} are the mutants with measurable TH at concentrations <5 mg/mL. Experiments were conducted using a custom−built nanoliter osmometer.

indistinguishable from the wild-type spectrum, and the spectra of the other mutants also displayed the characteristic double minimum at 205 and 222 nm seen for wild-type TmAFP, indicating that the secondary structure of the proteins was preserved.

Antifreeze Activity of TmAFP Mutants. The average TH activity of wild-type TmAFP was 1.8 °C at a concentration of 0.75 mg/mL, with hyperbolic dependence on protein concentration, in accordance with previous reports[32,35,40] (Figure 2). In contrast, most TmAFP mutants at a concentration of 1 mg/mL were unable to depress the freezing point below the melting point to a measurable extent, or to suppress dramatically the growth rate of a seed ice crystal relative to pure water, buffer, or solutions of nonantifreeze proteins. Exceptions were Y_{c-f} and V_{c-f}, with TH activity of 0.05 and 0.3 °C, respectively, at 1 mg/mL. (Figure 2). These measurements may be slightly biased by the difference in ice crystal size at the start of supercooling (∼25 μm along the c-axis in the presence of Y_{c-f} vs ∼15 μm along the c-axis in the presence of V_{c-f}), as larger crystals have more potential ice surface nucleation sites. With smaller crystals, greater TH activity may be obtainable for Y_{c-f}. Though lower than observed for wild-type TmAFP, TH activity values for Y_{c-f} and V_{c-f} are comparable to those measured for several other wild-type AFPs at similar w/v protein concentrations, for example, plant AFP from carrot,[41] type I AFPs from winter flounder[29] and shorthorn sculpin,[42] type II AFP from herring,[43] and type III AFPs.[44] Although ice crystal growth within the TH gap was not halted completely for the V_{c-f} mutant, the growth rate increased by a factor of 100 at the hysteresis freezing temperature, as described in more detail below. At much higher protein concentrations, marginal TH activity was observed for some of the other mutants. For example, N_{c-f} at 45 mg/mL showed TH activity of 0.03 °C; in this narrow window, crystal growth was not observed.

The behavior of ice crystals differed in the presence of Y_{c-f} compared to V_{c-f} both within the TH gap and at the freezing point. Y_{c-f} at a concentration of 2.5 mg/mL was able to halt the growth of ice crystals up to 0.1 °C below the equilibrium melting point. Even at Y_{c-f} concentrations that gave a TH of only 0.03 °C, ice crystal growth was not detected in this narrow TH gap. Specifically, for an ice crystal in a solution containing

1 mg/mL Y_{c-f}, growth could not be observed to a resolution of 1 μm over one hour. In the presence of Y_{c-f}, a mild "burst" was observed at the nonequilibrium freezing temperature, after which the crystal grew in the direction of the prism plane (Figure 5B and Supporting Information movie 1). This behavior is similar to wild-type TmAFP (Figure 5A), although the burst in the presence of the wild-type protein is more dramatic due to the lower freezing point (Figure 5A and Supporting Information movie 2). Experiments with dilute solutions of wild-type TmAFP (not shown) indicated that the behavior of ice crystals in the presence of Y_{c-f} is virtually indistinguishable from wild type at 2500-fold lower concentrations. Interestingly, although V_{c-f} showed greater TH activity than Y_{c-f} at equimolar protein concentrations, V_{c-f} did not completely arrest ice crystal growth within the TH gap (Figure 5C,D and Supporting Information movie 3). Nevertheless, a clear distinction was observed between the growth rates within the TH gap and after the burst, as mentioned above, as well as a dramatic reduction in crystal growth rate relative to the other mutants (except Y_{c-f}) at the same supercooling temperature (Figure 3A). For example, ice crystals formed in the presence of 1 mg/mL V_{c-f} at 0.07 °C supercooling grew to the direction of the a-axis at a rate of 0.09 μm/s, in comparison to a rate of 5.2 μm/s observed with 1 mg/mL H_{c-f}. When a temperature ramp of −0.01 °C every 4 s was applied to a seed ice crystal in the presence of V_{c-f}, the growth rate in the direction of the a-axis increased steadily and consistently with decreasing temperature, whereas growth in the c direction reached a maximum and then decreased (Figure 3B). When the temperature was lowered to the hysteresis freezing point or below, the growth rate increased significantly, and the crystal grew in a stepwise manner in all directions. Faceted steps were observed on the surface of the growing crystal (Figure 5C,D and Supporting Information movie 3). The temperature at which fast, stepwise crystal growth began was taken as the hysteresis freezing point. Our definition of the TH gap for V_{c-f} is consistent with previous studies in which ice crystal growth rates of less than 0.2 μm/s were considered to be within the TH gap.[45]

Ice Growth Morphology. The activity of the V_{c-f} and Y_{c-f} TmAFP mutants was also evident by the shapes of ice crystals grown in their presence. Ice crystals grown in dilute solutions of wild-type TmAFP exhibit hexagonal bipyramidal forms reminiscent of the shape of a lemon, as previously noted[4] (Figure 4B,C). The lemon shape was obtained during melting of ice crystals of all sizes tested (∼5−100 μm) in protein solutions at concentrations below 20 μM, even with as little as 0.1 μM (1 μg/mL) protein, when TH activity is too low to measure (<0.01 °C). At higher protein concentrations, faceting was not observed during melting, and the crystals melted into various anisotropic forms. When the temperature was steadily decreased, the crystal remained in its melting shape (i.e., lemon or anisotropic) through the entire hysteresis gap, until the nonequilibrium freezing point was reached.

Hexagonal lemon-like shapes were also observed during melting of Y_{c-f} solutions. However, as the temperature of the Y_{c-f} solution was lowered below T_m, the hexagonal bipyramid became faceted to form another hexagon 30° to the former, such that the final bipyramid contained 12 edges (Supporting Figure 1, Supporting Information). This shape was repeatedly obtained at all Y_{c-f} concentrations tested. The crystal was stable in this shape and did not grow or reform as the temperature was lowered further, until the hysteresis freezing point was reached and the crystal grew isotropically along the a-axis. The phenomenon of a 30° rotation between the growing and melting
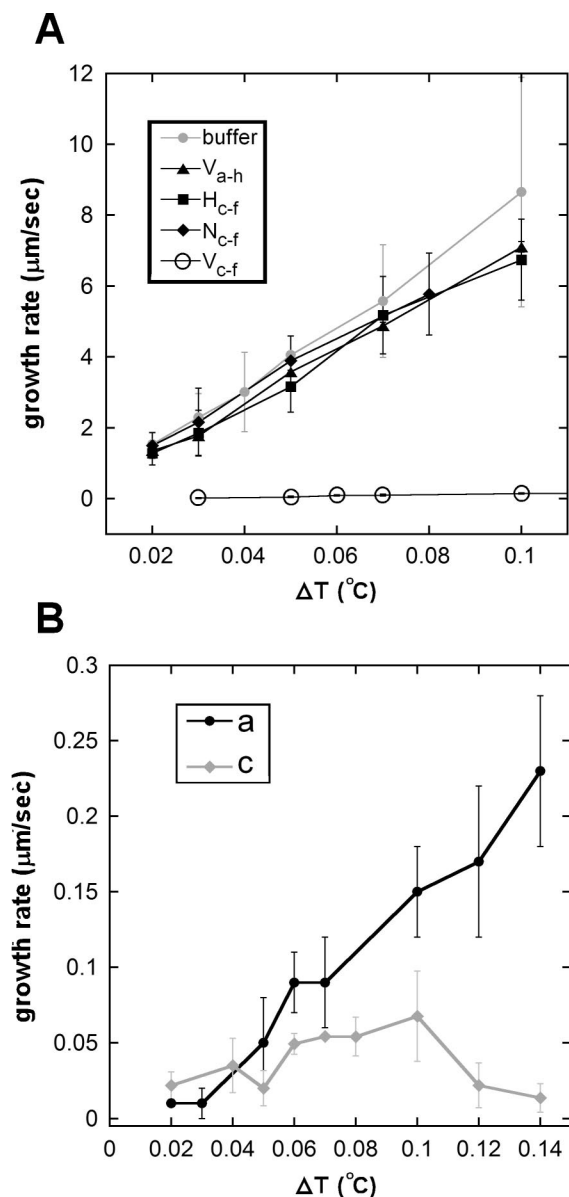
A

B

Figure 3. Growth rates of ice crystals in the presence of TmAFP mutants (1 mg/mL). The abscissa represents the supercooling temperature (the temperature below T_m). Each point represents the average and standard deviation of at least four independent experiments. (A) Growth rates of selected mutants in comparison to solution without protein. The ordinate is the rate of growth of a seed ice crystal radius (along the *a*-axis). V_{c-f} slows the growth rate of a seed ice crystal to nearly zero. (B) The dependence of ice crystal growth to the directions of the *a*- and the *c*-axes on the supercooling in the presence of V_{c-f}. For crystals grown in the presence of V_{c-f}, the rate of growth along the *a*-axis was calculated from the length of an edge of the hexagonal face.

planes was observed also with wild-type TmAFP at thousand-fold lower concentrations and with sbwAFP solution.[46] This relationship between growing and melting planes was also found in ice crystals under high pressure in water, and it was explained theoretically on the basis of the fast-growing direction also being the fast-melting direction.[47]

Ice crystals grown from V_{c-f} solutions were different from those grown with Y_{c-f} or wild-type TmAFP in several aspects. Lemon-like forms were observed during melting only when the crystal size was decreased to 20 μm or below, and even then they lasted not more than a few seconds (for 1 mg/mL protein solutions). Melting crystals were usually flat and round, similar
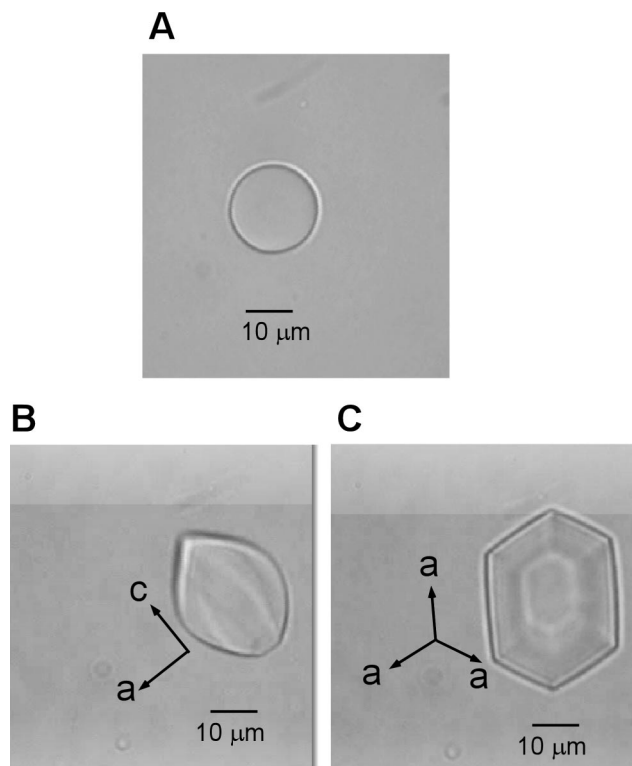
A

B   **C**

Figure 4. Ice crystal morphologies in the presence and absence of TmAFP. (A) Ice grown from pure water. (B, C) Ice grown in the presence of TmAFP, in different orientations. The Y_{c-f} mutant induced ice shapes similar to the wild−type protein.

to those obtained in water. As the temperature was lowered below the melting point, the crystals started to facet and formed hexagonal prisms, with more pronounced sharpening at lower temperatures (Figure 5C,D). The hexagonal crystal shape persisted during slow growth over a time range of hours, even when essentially the entire sample was frozen. In these cases, the sample drop became a single hexagonal crystal. We noted that at supercooling of around 0.05 °C below T_m (for 1 mg/mL V_{c-f} solution), the flat basal planes started to develop into hexagonal pyramids (Figure 5D, bottom left), but this phenomenon did not change the ice growth rates to any direction. At temperatures below the hysteresis freezing temperature, the growth rates increased substantially, and the crystal grew perpendicularly to all crystal facets, forming stepped ledges but maintaining hexagonal symmetry (Figure 5C,D and Supporting Information movie 3).

The presence of the X_{a-h} mutants, N_{c-f}, or H_{c-f}, did not have a significant effect on crystal habit at concentrations of 1 mg/mL. However, antifreeze characteristics are suggested for all these mutants by the sharpening of the crystals observed as the temperature is lowered below T_m (not shown). In most samples, the seed ice crystal faceted to a hexagonal shape immediately below T_m, but as the temperature was decreased, the facets disappeared and the crystals grew in the *a*-axis direction to form rounded disks indistinguishable from those observed in water or solutions without antifreeze proteins (Figure 4A). Although the changes in crystal morphology induced by these TmAFP mutants were minor, they were not observed when solutions containing control proteins (MBP, BSA, or Trx) were assayed even at relatively high concentrations (MBP, up to 4.3 mg/mL, BSA, up to 20 mg/mL, and Trx, up to 6.5 mg/mL). Ice crystals in the presence of any of the reference proteins melted and grew in a circular shape, as observed for pure water (Figure 4A). At
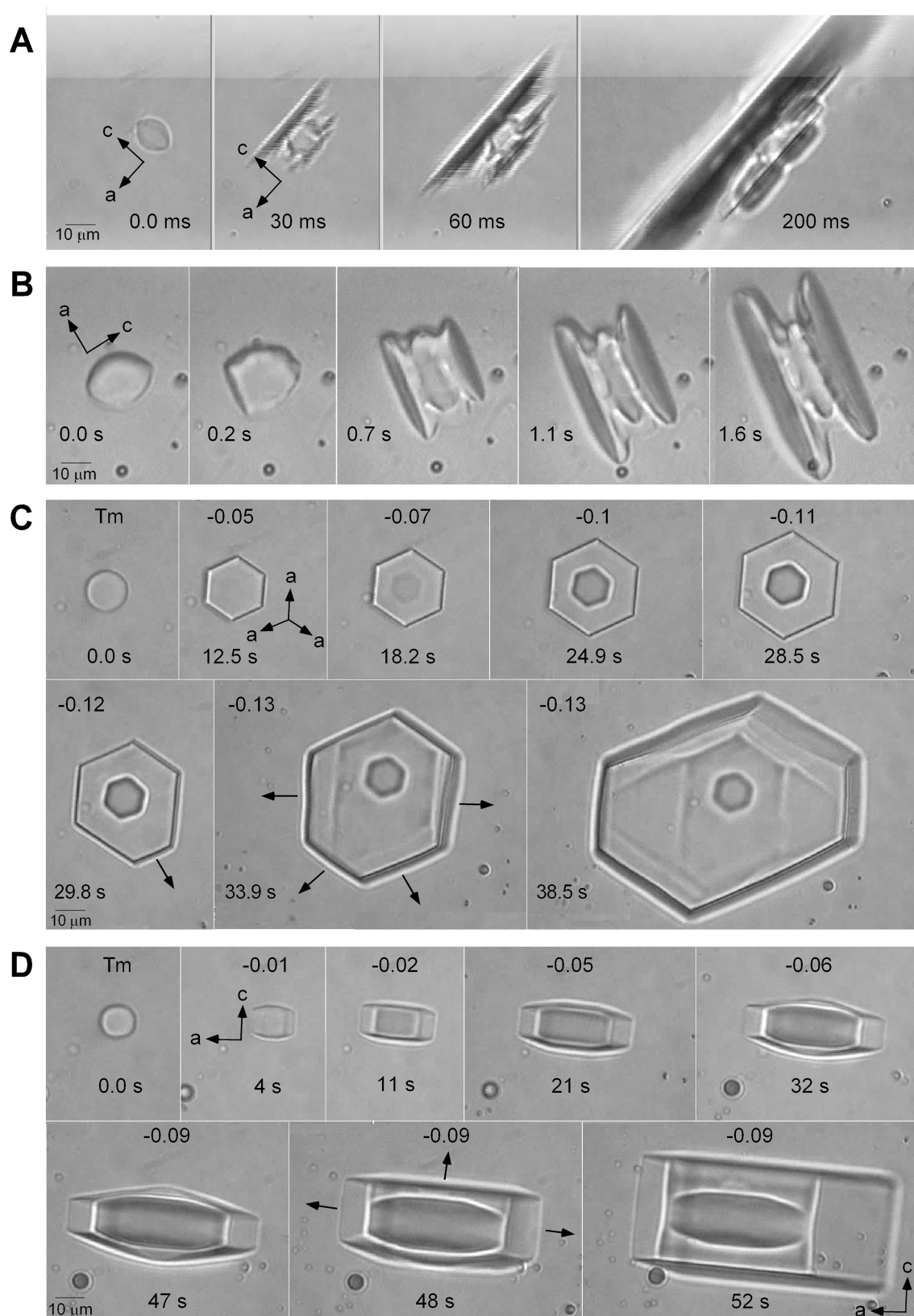
Figure 5. Bursts of ice crystals in the presence of wild-type and mutated TmAFPs. Time-lapse from the beginning of the burst (in milliseconds or seconds) is noted below each image. (A) Wild-type TmAFP (0.1 mg/mL). (B) Y_{c-f} (5 mg/mL). (C) V_{c-f} (0.1 mg/mL) oriented with the *c*-axis perpendicular to the page. The first five frames were taken during the temperature decline before the freezing point. At the hysteresis freezing point, stepped growth was observed (marked by arrows). The corresponding supercooling below T_m is noted in each frame. (D) As in C, but with a crystal oriented with the *a*-axis perpendicular to the page. Movies demonstrating ice growth with wild-type TmAFP, V_{c-f}, or Y_{c-f} in MPG format are available online as Supporting Information at http://pubs.acs.org/crystal. In the movies, the equilibrium melting temperature of the sample and the measured temperature in real time are displayed in the top left corner, and the real time is presented on the bottom.

relatively low temperatures (∼0.2 °C supercooling) some hexagonal growth could be detected also for the reference proteins, but ice reshaping at temperatures closer to T_m was detected only in the presence of the TmAFP mutants.

Discussion

The location of the TmAFP ice-binding face is apparent from the shape complementarity between the array of Thr side chain hydroxyls of the protein and the ice lattice. The regularity of the array is derived from the conformation of the TmAFP protein backbone, in particular, the distance between β-strands in the parallel β-sheet, the distance between Thr residues along each strand, and the flatness of the sheet containing these Thr residues. The relative positions of the relevant side chain functional groups are maintained by the rigidity of the structure, as observed by NMR.[48−50] Substitution of the Thr residues on the ice-binding face with other amino acids could in principle preserve the spacings observed in the wild-type protein and therefore the shape complementarity with ice. One may hypothesize that amino acid side chains sharing properties or functional groups in common with Thr may be compatible with antifreeze function if displayed uniformly on the TmAFP platform. A panel of TmAFP mutants with four or eight simultaneous and identical amino acid substitutions was designed to maintain the regularity of the ice-binding face array while varying its chemical properties.[33] A study of how such TmAFP variants interact with ice provides insight into the native ice-binding mechanism of highly regular hyperactive AFPs. Single amino acids substitutions on TmAFP[32] were previously used to assess the resilience of antifreeze activity to mutation and to define the ice-binding face of the protein. However, the repetitive character of the ice-binding face in these mutants was considerably disrupted, and the effect of single-site mutagenesis on ice binding was not investigated in the context of the ice-binding mechanism.

We observed in our studies that only the TmAFP mutants $V_{c−f}$ and $Y_{c−f}$ had significant residual TH activity, and the rest had no detectable TH activity at a concentration of 1 mg/mL. CD and NMR measurements demonstrated that the seven TmAFP mutants studied herein adopt a β-helical conformation similar to the wild type in solution. Furthermore, NMR experiments did not indicate oligomerization, even for $V_{a−h}$, which might be expected to self-associate due to hydrophobic interactions. A detailed spectroscopic analysis of the TmAFP mutants has been published elsewhere.[33] As these data imply that the TmAFP secondary and tertiary structures are preserved, the reduction in activity of the mutants is likely related to their chemical properties rather than to major defects in protein folding, with the caveat that minor structural changes could undermine the shape complementarity and radically affect antifreeze activity. The sensitivity of TH activity to mutagenesis contrasts with the robustness of the fold and indicates that non-Thr amino acids, even when provided in an array, are not functionally exchangeable for the native Thr.

There is no inherent reason why the amino acids chosen for our studies cannot participate in ice binding. For example, a model for a hyperactive calcium-dependent AFP from bacteria displays Thr and Asn residues on its ice-binding face in a repetitive arrangement,[9] albeit distributed differently from our $N_{c−f}$ construct. Other AFPs display various non-Thr residues, including hydrophobic, polar, and charged, on ice-interacting surfaces.[30,41,51,52] The TmAFP structure suggests that ice binding occurs through the Thr array and that the Thr hydroxyls are incorporated into the hydrogen bonding network of the ice

lattice. However, the importance of the hydroxyls in ice recognition has not been established. It is possible that the major factors in ice recognition are flatness and repetitiveness, in essence, the maximization of van der Waals interactions. Earlier mutagenesis studies conducted on the α-helical fish type I antifreeze peptide, in which the repetitive Thr residues on its ice-binding face were substituted with Val, Ser, and allo-Thr, showed that loss of the methyl groups was more deleterious to TH activity than loss of a hydroxyl by substituting it with a second methyl group.[26−28] Indeed, when all four Thr residues in its ice-binding array were substituted with Val, the mutated protein (VVVV2KE) retained 30−50% of its TH activity, although there are contradicting results regarding whether crystal growth was completely arrested or continued at a slow rate.[27,28] Apparently, other natural and mutant AFPs exhibit measurable TH activity with arrays of amino acids aside from or in addition to Thr.

In the case of fish type I AFP, hydrophobic effects appeared to be more important than hydrogen bonding in promoting ice association. In contrast, our comparable TmAFP mutant, in which 8 out of 11 Thr residues were substituted with Val ($V_{a−h}$), was inactive. This observation suggests that the factors contributing to the TH activity of hyperactive insect AFPs differ from those that underlie the TH activities of moderate AFPs. The structural similarity of $V_{a−h}$ to wild-type TmAFP, as well as the similarity in size and shape of the Val and Thr side chains, suggests that this mutant potentially has the same high shape complementarity to ice as the wild-type protein. Furthermore, Val is more hydrophobic than Thr. The hydrophobicity of AFP ice-binding faces favors incorporation of AFP molecules into the interfacial region between ice and water, and higher hydrophobicity is associated with decreased solubility and increased affinity to ice.[17] If hydrophobic interactions of the γ-methyl groups with ice were a sufficient driving force for adsorption, we would expect this mutant to retain some TH activity or at least to induce ice faceting during growth or melting. The complete impotence of $V_{a−h}$ suggests that hydrophobic interactions are insufficient for ice binding by TmAFP. This finding is in marked contrast to mutation studies conducted on α-helical type I flounder AFP.[27,28]

There is clearly an essential role for the Thr hydroxyl groups in the mechanism of TmAFP, and they may participate at several stages in organization of the interaction with ice. Even before contact with ice, the hydroxyls may help preorient the side chains in appropriate rotamers by hydrogen bonding to the protein backbone.[50,53] The rotamers adopted by the Val residues in the $V_{a−h}$ mutant may not be similarly restricted, disrupting the match to the ice lattice. Spectroscopic studies of the mutants did not specifically address this issue. Another role for hydroxyls may be binding the file of water molecules on the ice-binding face of wild-type TmAFP. This water file is presumably absent in $V_{a−h}$ due to the lack of hydroxyls available for hydrogen bonding. The ordered water molecules putatively participate in the solidification of the protein to the ice,[21] and their lack might prevent irreversible binding. Finally, and most obviously, the Thr hydroxyls themselves may be essential for ice binding.

TmAFP mutants that did show at least minimal activity were from the $X_{c−f}$ mutant series. Despite the reduced activity compared to wild type, the $V_{c−f}$ and $Y_{c−f}$ mutants, unlike other mutants, clearly retained TH activity even at sub-millimolar protein concentrations. This activity may be due to the seven nonmutated Thr residues on the ice-binding face present in all $X_{c−f}$ mutants, which can in principle associate with ice as in wild-type TmAFP. This explanation then raises the question of

why V_{c-f} and Y_{c-f} show TH activity at 1 mg/mL and H_{c-f} and N_{c-f} do not. The Val and Tyr side chains may contribute positively to ice binding compared to His or Asn, or these side chains may be less disruptive to the overall structure, backbone flexibility, and function of the non-mutated part of the ice-binding face. The observation that V_{c-f} and Y_{c-f} are more similar than H_{c-f} and N_{c-f} to wild-type TmAFP in their CD spectra suggests that Val and Tyr mutations permit some functionality because they have less of an impact on TmAFP structure or dynamics. Possible specific effects of Tyr vs Val will be discussed below. Notably, when the number of Thr residues on the TmAFP ice-binding face was reduced from 11 to 8 by deleting a coil from the β-helix,[54] a drop in TH activity from about 3.5° to about 1° was observed at 1 mg/mL protein, as compared to a drop from about 2° for wild type to about 0.3° for V_{c-f} in our experiments. The significant decrease in activity seen in both studies despite preservation of most of the ice-binding face likely reflects the cooperativity of the fold in aligning the Thr residues, as well as the cooperativity between Thr side chains in function of hyperactive AFPs.[54]

Both V_{c-f} and Y_{c-f} have a well-folded backbone and preserve the same number of native Thr residues, yet these mutants have differences in activity that further illuminate the mechanism of action of TmAFP. V_{c-f} cannot arrest the growth of an ice crystal, whereas Y_{c-f} can (see supporting movies). Furthermore, these two mutants induce different ice shapes from one another during growth and during melt. These differences perhaps arise from the distinct interactions each mutant forms with ice and may be caused by contributions from the Val and Tyr residues themselves, rather than due to indirect effects on the remaining Thr residues of the ice-binding face. Although the significant reduction in TH activity of V_{c-f} and Y_{c-f} is probably associated with disruption of the regularity of the array and the shape complementarity of their ice-binding faces, we suggest that the differences between these mutants are related not only to the size of the Val and Tyr side chains but also to the hydrophobic and hydrophilic characters of the proteins.

A role for both hydrophobic and hydrophilic moieties in promoting TH activity was suggested by several studies on type I and type III fish AFPs[26,27,31] and discussed in the model of Kristiansen and Zachariassen.[17] These authors suggested a two-step mechanism for AFP interaction with ice. According to their hypothesis, the first step, which takes place at the equilibrium melting temperature, is equilibrium distribution of AFP molecules between the bulk solution and the interfacial region of ice and water. An effective distribution relies on limited solubility of the AFP. The second step occurs when the temperature is lowered below the equilibrium melting point, and the interfacial region under the AFP crystallizes. Because of the particular characteristics of AFP that distinguish it from other solutes, the protein "solidifies" onto the ice surface rather than being excluded by the expanding ice. The solidification process includes formation of crystal facets and generation of strong interactions between the protein surface and water molecules from the ice lattice, which is necessary to prevent exclusion of protein molecules from the surface and to ensure irreversible protein adsorption to ice. The two steps in the mechanism are dominated by distinct forces. The entropic gain upon removal of hydrophobic residues from bulk water favors partitioning of AFP molecules into the ice–water interfacial region, and this process determines the concentration of protein on the ice surface. In the second step, which is affected by shape complementarity between AFP and ice planes, hydrophilic

interactions as well are required for permanent attachment of the AFPs to ice.

This theory can be expanded to the establishment of surface protein density not only at the T_m but also at temperatures below the bulk melting point. At temperatures in the TH gap, the curved ice surface is at equilibrium with the surrounding water, and it is stabilized by perseveringly adhered AFP molecules that are assumed to be "locked" onto the ice surface.[17] This surface can adsorb additional AFP molecules reversibly. In the rare events of engulfment or detachment of a locked molecule, local growth occurs, which can be arrested by another adsorbed AFP molecule that in turn becomes locked onto the surface. The typical distance between the adsorbed AFP molecules and the dynamics of forming stable bonds with the ice determine the limit of supercooling that this process can support and thus the TH gap.

The elaborated mechanism of Kristiansen and Zachariassen can be useful for interpretation of the changes in ice crystal morphologies and growth habits observed in the presence of V_{c-f} and Y_{c-f}. The hydrophobic ice-binding face of V_{c-f} presumably decreases the solubility of the protein, favoring partitioning out of bulk water due to the hydrophobic effect. The outcome is reversible adsorption to the ice lattice, and as the temperature drops the crystal is faceted, in accordance with completion of the first step of the ice binding. However, the deficiency of hydroxyl groups in V_{c-f} may undermine the second step in the mechanism and allow dissociation from the ice. The observation that ice continues to grow in the presence of V_{c-f}, albeit at a dramatically reduced rate compared to in buffer alone, further indicates that binding of this mutant is reversible. The observed dependence of the crystal growth rate on the degree of supercooling is presumably due to the temperature-dependence of the rate of incorporation of water into the ice lattice upon dissociation of the mutant AFP. Whether this incorporation of water is the cause or effect of protein dissociation is not known. The observed maximum in ice growth velocity in the c-axis direction may stem from intrinsic kinetic properties of ice growth independent of AFPs.[55]

In the case of Y_{c-f}, the hydroxyl groups of the Tyr side chains may in principle form hydrogen bonds with the ice lattice and lock protein molecules onto the ice surface, which would explain the ability of Y_{c-f} to halt ice growth completely despite the low TH activity. Furthermore, ice crystals in the presence of Y_{c-f} are lemon-shaped and burst perpendicular to the c-axis, as seen in the presence of wild–type TmAFP. These observations suggest that stable adsorption of Y_{c-f} does occur, and the low TH activity may be the outcome of fewer protein molecules bound to the ice surface. It is not likely that this loss of activity is due to higher solubility of this mutant relative to wild-type TmAFP since Tyr is more hydrophobic than Thr. Nevertheless, the density of Y_{c-f} molecules locked on the ice surface is expected to be low due to decreased shape complementarity. The increased distance between protein molecules on the ice surface would lead to reduction in TH activity due to increased critical radius at the convex zone between bound proteins,[17] in spite of the strong binding of Y_{c-f} to the ice and in accordance with the model mechanism.

Further evidence for the distinct characters of the Y_{c-f} and V_{c-f} activities is the morphology of ice obtained with each of these mutants. Modification of ice crystal shape is a defining characteristic of AFPs, as the interactions of AFPs with ice occur at specific ice crystal planes. A seed ice crystal in slightly supercooled water or in dilute solutions grows in the shape of a round disk, with only the basal plane faceted. Faceting of the

prism faces occurs at high pressure (>1600 bar) and low temperatures (< -16 °C).[56] Faceting of any but the basal planes of ice obtained at atmospheric pressure and slight supercooling indicates the presence of a substance that interacts with specific ice planes.[28,46] The observation that Y_{c-f} shapes ice into lemon-like bipyramids during melt and into disklike shapes after burst, similar to wild-type TmAFP, suggests that Y_{c-f} interacts with ice through the same planes as the wild-type protein. This assumption, nevertheless, needs to be verified experimentally. On the other hand, crystals grown in the presence of V_{c-f} are shaped as hexagonal prisms, and when the temperature is close to the bulk melting point, hexagonal corners are formed along the c direction. Furthermore, the crystal burst is to the a direction with Y_{c-f} and with wild-type TmAFP, and to both the a and the c directions in the presence of V_{c-f}. This result suggests that V_{c-f} has lower affinity to the basal plane relative to Y_{c-f} and to wild type. Basal plane affinity may be unique to the hyperactive AFPs such as TmAFP and thus responsible for their hyperactivity.[1,22,57] The putative higher affinity to the basal plane of Y_{c-f} relative to V_{c-f} might indicate the importance of hydrogen bonds for the interaction of TmAFP with the basal planes of ice.

Reduced TH activity of AFP mutants associated with slow crystal growth and changes in crystal morphologies was previously reported for other antifreeze mutants[30,45,58–60] and ascribed to low affinity of these mutants to ice relative to the wild-type protein.[45] Two alternative models were provided to account for the changes in crystal morphology. One is that AFPs have affinity to more than one crystal plane, and reducing the affinity of the mutants to certain planes results in crystals with different $c{:}a$ axis ratios. The second is that prevention of ice growth occurs plane by plane. The AFPs bind to the prism planes and block water in this direction, but water can still join the basal planes such that new prism planes are formed. The competition between generation of new prism planes and the binding of AFPs to these planes determines the $c{:}a$ axis ratio.[45] An analogous competition can be envisaged for AFPs that bind basal planes. If TmAFP mutants with reduced activity bind to a single plane, one would expect them to shape ice into bipyramidal crystals. However, crystals in the presence of V_{c-f} were always hexagonal prisms rather than bipyramidal, suggesting that V_{c-f}, like wild-type TmAFP, binds more than one plane, but perhaps with reduced affinity to both. It is also possible that V_{c-f} has developed affinity to other ice planes, giving rise to the different morphologies of ice. Interestingly, the morphology of ice crystals in the presence of the type I AFP VVVV2KE mutant below the hysteresis freezing temperature was similar to the wild type,[28] supporting the proposal that substitution with Val in TmAFP alters an aspect of the ice-binding mechanism not featured in type I fish AFP.

The ice-binding face of wild-type TmAFP is an orderly array of Thr side chains that act in concert to bind strongly to ice. Apart from the aspects of hydrophobicity, hydrophilicity, and geometrical complementarity, the cooperativity of these Thr functional groups may be crucial for the antifreeze properties of this protein, in particular accounting for its hyperactivity. First, interactions between individual Thr side chains and the ice grid are mutually strengthened by the proper positioning of the others. Second, various types of interactions may cooperate to support each other. For example, hydrophobic interactions may exclude bulk water and increase the enthalpic contribution of hydrogen bonds with ice.[51] From this perspective, it is not surprising that division or diminishment of the cooperative system disables hyperactivity. It should be emphasized that,

despite the poor activity of these mutants relative to wild-type TmAFP, they show similar molar TH activities as wild-type fish type I AFPs.

Conclusions

The disulfide-rich β-helix structure of TmAFP sustains multiple substitutions of the threonines on its ice-binding face without disruption of its integrity. Here we used multiple substitutions to investigate how changes in the functional groups arrayed on the TmAFP surface impact ice-binding activity. The TH activity, ice growth rates, and ice crystal shapes in the presence of the mutants indicate that Thr residues are uniquely suited to provide antifreeze hyperactivity. Low but significant TH activity was measured for two mutants, those with four Val residues or four Tyr residues in place of Thr in the center of the TmAFP ice-binding face. Our results are consistent with the model that combines equilibrium adsorption of AFP molecules to the ice with strong hydrogen bonding. Analysis of our two active mutants illuminates aspects of the ice-binding mechanism of AFPs. Hydrophobic interactions may contribute to association of TmAFP with ice, but they are not sufficient to support the tight adsorption proposed to block crystal growth within the TH gap. The antifreeze activity of TmAFP is thus a combination of reversible and irreversible binding to ice. The reversible binding is supported by hydrophobic interactions, but hydrogen bonds might be necessary for the irreversible binding. Although mutations in the ice-binding face lead to reduced thermal hysteresis activity, disruption of different aspects of the ice-binding mechanism lead to different phenotypes that can be distinguished by the behavior of ice crystals.

Supporting Information Available: Figure of 30° difference between the growing and the melting planes of crystals in the presence of Y_{c-f}. Movies 1–3 of ice growth in the presence of TmAFP, V_{c-f} and Y_{c-f}, respectively (see Figure 5 legend for details). This material is available free of charge via the Internet at http://pubs.acs.org.

References

(1) Scotter, A. J.; Marshall, C. B.; Graham, L. A.; Gilbert, J. A.; Garnham, C. P.; Davies, P. L. *Cryobiology* **2006**, *53* (2), 229–39.
(2) Tyshenko, M. G.; Doucet, D.; Davies, P. L.; Walker, V. K. *Nat. Biotechnol.* **1997**, *15* (9), 887–90.
(3) Marshall, C. B.; Fletcher, G. L.; Davies, P. L. *Nature* **2004**, *429* (6988), 153.
(4) Graham, L. A.; Liou, Y. C.; Walker, V. K.; Davies, P. L. *Nature* **1997**, *388* (6644), 727–8.
(5) Jia, Z.; Davies, P. L. *Trends Biochem. Sci.* **2002**, *27* (2), 101–6.
(6) Marshall, C. B.; Chakrabartty, A.; Davies, P. L. *J. Biol. Chem.* **2005**, *280* (18), 17920–9.
(7) Duman, J. G.; Li, N.; Verleye, D.; Goetz, F. W.; Wu, D. W.; Andorfer, C. A.; Benjamin, T.; Parmelee, D. C. *J. Comp. Physiol. B* **1998**, *168* (3), 225–32.
(8) Graham, L. A.; Davies, P. L. *Science* **2005**, *310* (5747), 461.
(9) Garnham, C. P.; Gilbert, J. A.; Hartman, C. P.; Campbell, R. L.; Laybourn-Parry, J.; Davies, P. L. *Biochem. J.* **2008**, *411* (1), 171–80.
(10) Raymond, J. A.; DeVries, A. L. *Proc. Natl. Acad. Sci. U. S. A.* **1977**, *74* (6), 2589–93.
(11) Knight, C.; Wierzbicki, A. *Cryst. Growth Des.* **2001**, *1* (6), 439–46.
(12) Sander, L. M.; Tkachenko, A. V. *Phys. Rev. Lett.* **2004**, *93* (12), 128102.

(13) Pertaya, N.; Marshall, C. B.; DiPrinzio, C. L.; Wilen, L.; Thomson, E. S.; Wettlaufer, J. S.; Davies, P. L.; Braslavsky, I. *Biophys. J.* **2007**, *92* (10), 3663–73.

(14) Beaglehole, D.; Wilson, P. *J. Phys. Chem.* **1993**, *97* (42), 11053–55.

(15) Wierzbicki, A.; Dalal, P.; Cheatham, T. E., 3rd; Knickelbein, J. E.; Haymet, A. D.; Madura, J. D. *Biophys. J.* **2007**, *93* (5), 1442–51.

(16) Li, Q. Z.; Yeh, Y.; Liu, J. J.; Feeney, R. E.; Krishnan, V. V. *J. Chem. Phys.* **2006**, *124* (20), 204702.

(17) Kristiansen, E.; Zachariassen, K. E. *Cryobiology* **2005**, *51* (3), 262–80.

(18) Knight, C. A.; Cheng, C. C.; DeVries, A. L. *Biophys. J.* **1991**, *59* (2), 409–18.

(19) Wen, D.; Laursen, R. A. *Biophys. J.* **1992**, *63* (6), 1659–62.

(20) Knight, C. A.; Driggers, E.; DeVries, A. L. *Biophys. J.* **1993**, *64* (1), 252–9.

(21) Liou, Y. C.; Tocilj, A.; Davies, P. L.; Jia, Z. *Nature* **2000**, *406* (6793), 322–4.

(22) Graether, S. P.; Kuiper, M. J.; Gagne, S. M.; Walker, V. K.; Jia, Z.; Sykes, B. D.; Davies, P. L. *Nature* **2000**, *406* (6793), 325–8.

(23) DeVries, A. L.; Lin, Y. *Biochim. Biophys. Acta* **1977**, *495* (2), 388–92.

(24) DeVries, A. L. *Phil. Trans. R. Soc. Lond. B* **1984**, *304*, 575–88.

(25) Wen, D.; Laursen, R. A. *J. Biol. Chem.* **1992**, *267* (20), 14102–8.

(26) Chao, H.; Houston, M. E., Jr.; Hodges, R. S.; Kay, C. M.; Sykes, B. D.; Loewen, M. C.; Davies, P. L.; Sonnichsen, F. D. *Biochemistry* **1997**, *36* (48), 14652–60.

(27) Zhang, W.; Laursen, R. A. *J. Biol. Chem.* **1998**, *273* (52), 34806–12.

(28) Haymet, A. D.; Ward, L. G.; Harding, M. M.; Knight, C. A. *FEBS Lett.* **1998**, *430* (3), 301–6.

(29) Baardsnes, J.; Kondejewski, L. H.; Hodges, R. S.; Chao, H.; Kay, C.; Davies, P. L. *FEBS Lett.* **1999**, *463* (1−2), 87–91.

(30) Baardsnes, J.; Jelokhani−Niaraki, M.; Kondejewski, L. H.; Kuiper, M. J.; Kay, C. M.; Hodges, R. S.; Davies, P. L. *Protein Sci.* **2001**, *10* (12), 2566–76.

(31) Sonnichsen, F. D.; DeLuca, C. I.; Davies, P. L.; Sykes, B. D. *Structure* **1996**, *4* (11), 1325–37.

(32) Marshall, C. B.; Daley, M. E.; Graham, L. A.; Sykes, B. D.; Davies, P. L. *FEBS Lett.* **2002**, *529* (2−3), 261–7.

(33) Bar, M.; Scherf, T.; Fass, D. *Protein Eng. Des. Sel.* **2008**, *21* (2), 107–14.

(34) Schwede, T.; Kopp, J.; Guex, N.; Peitsch, M. C. *Nucleic Acids Res.* **2003**, *31* (13), 3381–5.

(35) Bar, M.; Bar−Ziv, R.; Scherf, T.; Fass, D. *Protein Expr. Purif.* **2006**, *48* (2), 243–52.

(36) Kapust, R. B.; Waugh, D. S. *Protein Expr. Purif.* **2000**, *19* (2), 312–8.

(37) Gross, E.; Sevier, C. S.; Heldman, N.; Vitu, E.; Bentzur, M.; Kaiser, C. A.; Thorpe, C.; Fass, D. *Proc. Natl. Acad. Sci. U. S. A.* **2006**, *103* (2), 299–304.

(38) Chakrabartty, A.; Hew, C. L. *Eur. J. Biochem.* **1991**, *202* (3), 1057–63.

(39) Choi, Y. E. *A Study on Hyperactive Antifreeze Proteins from the Insect Tenebrio molitor*; Ohio University, Athens, 2007, http://www.ohiolink.edu/etd/view.cgi?acc_num=ohiou1195953014.

(40) Liou, Y. C.; Daley, M. E.; Graham, L. A.; Kay, C. M.; Walker, V. K.; Sykes, B. D.; Davies, P. L. *Protein Expr. Purif.* **2000**, *19* (1), 148–57.

(41) Zhang, D. Q.; Liu, B.; Feng, D. R.; He, Y. M.; Wang, S. Q.; Wang, H. B.; Wang, J. F. *Biochem. J.* **2004**, *377* (Pt 3), 589–95.

(42) Fairley, K.; Westman, B. J.; Pham, L. H.; Haymet, A. D.; Harding, M. M.; Mackay, J. P. *J. Biol. Chem.* **2002**, *277* (27), 24073–80.

(43) Li, Z.; Xiong, F.; Lin, Q.; d'Anjou, M.; Daugulis, A. J.; Yang, D. S.; Hew, C. L. *Protein Expr. Purif.* **2001**, *21* (3), 438–45.

(44) Sonnichsen, F. D.; Sykes, B. D.; Chao, H.; Davies, P. L. *Science* **1993**, *259* (5098), 1154–7.

(45) DeLuca, C. I.; Chao, H.; Sonnichsen, F. D.; Sykes, B. D.; Davies, P. L. *Biophys. J.* **1996**, *71* (5), 2346–55.

(46) Pertaya, N.; Celik, Y.; DiPrinzio, C. L.; Wettlaufer, J. S.; Davies, P. L.; Braslavsky, I. *J. Phys.: Condens. Matter* **2007**, *19* (41), 412101.

(47) Cahoon, A.; Maruyama, M.; Wettlaufer, J. S. *Phys. Rev. Lett.* **2006**, *96* (25), 255502.

(48) Daley, M. E.; Spyracopoulos, L.; Jia, Z.; Davies, P. L.; Sykes, B. D. *Biochemistry* **2002**, *41* (17), 5515–25.

(49) Daley, M. E.; Sykes, B. D. *J. Biomol. NMR* **2004**, *29* (2), 139–50.

(50) Daley, M. E.; Sykes, B. D. *Protein Sci.* **2003**, *12* (7), 1323–31.

(51) Baardsnes, J.; Davies, P. L. *Biochim. Biophys. Acta* **2002**, *1601* (1), 49–54.

(52) Li, Z.; Lin, Q.; Yang, D. S.; Ewart, K. V.; Hew, C. L. *Biochemistry* **2004**, *43* (46), 14547–54.

(53) Dunbrack, R. L., Jr.; Karplus, M. *Nat. Struct. Biol.* **1994**, *1* (5), 334–40.

(54) Marshall, C. B.; Daley, M. E.; Sykes, B. D.; Davies, P. L. *Biochemistry* **2004**, *43* (37), 11637–46.

(55) Shimada, W.; Furukawa, Y. *J. Phys. Chem. B* **1997**, *101* (32), 6171–3.

(56) Maruyama, M. *J. Cryst. Growth* **2005**, *275* (3−4), 598–605.

(57) Pertaya, N.; Marshall, C. B.; Celik, Y.; Davies, P. L.; Braslavsky, I. *Biophys. J.* **2008**, *95* (1), 333–341.

(58) Chakrabartty, A.; Yang, D. S.; Hew, C. L. *J. Biol. Chem.* **1989**, *264* (19), 11313–6.

(59) Tachibana, Y.; Fletcher, G. L.; Fujitani, N.; Tsuda, S.; Monde, K.; Nishimura, S. *Angew. Chem., Int. Ed. Engl.* **2004**, *43* (7), 856–62.

(60) Loewen, M. C.; Gronwald, W.; Sonnichsen, F. D.; Sykes, B. D.; Davies, P. L. *Biochemistry* **1998**, *37* (51), 17745–53.